KI REPORTS
KIReports.org
TRANSLATIONAL RESEARCH

High Macrophage Densities in Native Kidney Biopsies Correlate With Renal Dysfunction and Promote ESRD

Maren B. Pfenning[1,2,9], Jessica Schmitz[1,9], Irina Scheffner[3], Kevin Schulte[4], Abedalrazag Khalifa[1], Hossein Tezval[5], Alexander Weidemann[6], Anke Kulschewski[7], Ulrich Kunzendorf[4], Sebastian Dietrich[4], Hermann Haller[3], Jan T. Kielstein[8], Wilfried Gwinner[3] and Jan H. Bräsen[1]

[1]Nephropathology Unit, Institute of Pathology, Hannover Medical School, Hannover, Lower Saxony, Germany; [2]Medical Department I, Gastroenterology, Hepatology and Nephrology, Clinics Passau, Passau, Bavaria, Germany; [3]Clinic for Kidney and Hypertension Diseases, Hannover Medical School, Hannover, Lower Saxony, Germany; [4]Clinic for Nephrology and Hypertension, Christian-Albrechts-University, University Hospital Schleswig-Holstein, Campus Kiel, Kiel, Schleswig-Holstein, Germany; [5]Department of Urology and Urological Oncology, Hannover Medical School, Hannover, Lower Saxony, Germany; [6]Medical Clinic III – Nephrology and Dialysis, St. Vinzenz Hospital, Paderborn, North Rhine-Westphalia, Germany; [7]Clinic for Nephrology and Hypertension, University Hospital Oldenburg, Oldenburg, Lower Saxony, Germany; and [8]Medical Clinic V, Nephrology, Rheumatology and Blood Purification, Academic Teaching Hospital Braunschweig, Braunschweig, Lower Saxony, Germany

Introduction: Macrophages and monocytes are main players in innate immunity. The relevance of mononuclear phagocyte infiltrates on clinical outcomes remains to be determined in native kidney diseases.

Methods: Our cross-sectional study included 324 patients with diagnostic renal biopsies comprising 17 disease entities and normal renal tissues for comparison. All samples were stained for $CD68^+$ macrophages. Selected groups were further subtyped for $CD14^+$ monocytes and $CD163^+$ alternatively activated macrophages. Using precise pixel-based digital measurements, we quantified cell densities as positively stained areas in renal cortex and medulla as well as whole renal tissue. Laboratory and clinical data of all cases at the time of biopsy and additional follow-up data in 158 cases were accessible.

Results: Biopsies with renal disease consistently revealed higher $CD68^+$-macrophage densities and $CD163^+$-macrophage densities in cortex and medulla compared to controls. High macrophage densities correlated with impaired renal function at biopsy and at follow-up in all diseases and in diseases analyzed separately. High cortical $CD68^+$-macrophage densities preceded shorter renal survival, defined as requirement of permanent dialysis. $CD14^+$ monocyte densities showed no difference compared to controls and did not correlate with renal function.

Conclusion: Precise quantification of macrophage densities in renal biopsies may contribute to risk stratification to identify patients with high risk for end-stage renal disease (ESRD) and might be a promising therapeutic target in renal disease.

Kidney Int Rep (2023) **8,** 341–356; https://doi.org/10.1016/j.ekir.2022.11.015
KEYWORDS: Dialysis risk; Digital pathology; Disease progression; Macrophage; Native kidney disease; Renal pathology

See Commentary on Page 212

Renal damage is caused by a variety of genetic, immunologic, metabolic, cardiovascular, and infectious factors. Eventually, most of them can lead to renal function decline, caused by irreversible interstitial fibrosis and scarring[1] because of persistent inflammation with continuous injury and pathologic wound healing.[2,3] Moreover, there are strong indications for a pathogenetic relationship between acute kidney injury (AKI) and chronic kidney disease (CKD); acute renal damage causes inflammation, which in turn damages the kidney, nurturing fibrosis and thus promoting long-term function decline.[4]

Macrophages and monocytes play critical roles in innate immunity. The main tasks of macrophages are heterogenous because of their high plasticity, and

Correspondence: Jan Hinrich Bräsen, Nephropathology Unit, Institute of Pathology, Hannover Medical School, OE 5110, Carl-Neuberg-Str. 1, 30625 Hannover, Germany. E-mail: Braesen.Jan@mh-hannover.de

[9]MBP and JS contributed equally

Received 1 November 2022; accepted 21 November 2022; published online 29 November 2022

include host defense, inflammation, maintaining homeostasis, and restoring tissue integrity.[5] Despite macrophages' known low specificity for antigens, their ability for independent allorecognition and trained immunity through epigenetic, transcriptional, and functional reprogramming has been shown in infections, vaccination, and solid organ transplantation.[6,7] The plasticity of macrophages is reflected in their ability to switch phenotype depending on the tissue micromilieu. Historically, a systematic classification for phenotypic diversity of extreme M1/M2 types was first introduced by Mills *et al*.[8] This approach was based on different metabolic states of murine macrophages, as follows: M1 represents the classically ("aggressive") and M2 the alternatively activated ("protective") macrophages. However, controversy remains regarding the relevance and nomenclature in humans,[9] because substantial differences exist between human diseases and animal models.[10,11] Recent research suggests a model of a rather continuous spectrum of phenotypes modified by stimuli of microenvironment.[12,13] Genetic modifications and transcriptional regulations can be used for subtype distinction[14]; however, markers of different activation states of macrophages in paraffin-embedded human tissues are scarce; especially, common M1 markers, CD80, CD81, and CD86, do not work in paraffin. Human leukocyte antigen–DR isotope can be used with double-staining methods, but with this technique the stain is still problematic to interpret.[15] Macrophages are easily overlooked in routine pathologic tissue sections if not specifically stained. Therefore, the present study focused on a rough characterization of polarization, applying CD68 as pan-macrophage marker and CD163 for alternatively activated (M2) macrophages. CD14 was used to visualize monocytes and blood-born "monocytic" macrophages, which were derived from monocytes and were recruited from blood into tissue where they differentiate to macrophages.[16,17]

Our multicentric cross-sectional study aimed at quantifying macrophages and monocytes in various human native kidney diseases for comparison. We quantified macrophages infiltration using a precise pixel-based digital measurement in diseased renal biopsies and normal tissues to determine their contribution to common renal diseases and functional outcome.

METHODS

Patients

Our retrospective cross-sectional study was approved by the local ethics committee (MHH 3516-2017). We included 324 patients with native kidney diseases who underwent diagnostic renal biopsies between 2014 and 2018 in 13 hospitals in Northern Germany. Additional normal kidney tissues from 9 tumor nephrectomies were used as controls. On the basis of histologic and clinical diagnoses, patients were grouped into 17 disease entities (Table 1).

Subgroups

The group of small vessel vasculitis (SVV) or pauci-immune crescentic glomerulonephritis was further divided into subgroups according to antineutrophil cytoplasmic antibody (ANCA)-status and disease activity. Twenty-one (42%) SSV-patients met the diagnostic criteria for pANCA$^+$-microscopic polyangiitis, 20 (40%) SSV-patients were diagnosed with cANCA$^+$-granulomatosis with polyangiitis, 5 (10%) patients presented with ANCA-negative vasculitis, and 4 (8%) patients had a nonactive form of vasculitis (i.e., previously diagnosed vasculitis showing only AKI without morphologic signs of SVV-activity).

Data

The medical history of all patients was filed, including physical examination and laboratory data (blood and urine) recorded during the hospitalization period during which the biopsies were taken. In 158 cases, additional clinical follow-up data were accessible spanning 20 to 1,675 (median 293.5) days after biopsy. Renal function (eGFR, estimated glomerular filtration rate) was estimated by the CKD Epidemiology Collaboration formula.[18] Renal function was categorized according to CKD nomenclature of Kidney Disease–Improving Global Outcomes[19] and AKI-stages were defined with Risk, Injury, Failure, Loss, and End-stage Kidney criteria.[20]

Histology

A total of 324 biopsies (1 per patient) were analyzed: The cases included were nonselected; during a certain time period, every biopsy taken from native kidneys received an additional immunostain for macrophages (clone PGM1). There were no inclusion criteria. Archival routine stainings (hematoxylin and eosin-Elastica, periodic acid-Schiff reaction series, Jones methenamine with or without hematoxylin and eosin-double stain, Sirius red, immunohistochemistry: IgA, IgG, IgM, C1q, C3c, kappa, and lambda light chain) were re-evaluated including electron microscopy and classifications for SVV (histopathologic classification of Berden[21] and Brix renal risk score[22]) and IgA nephritis (IgAN; Oxford-Classification[23]). Automated immunohistochemistry (Ventana Ultra; Ventana Medical Systems Inc., Tucson, AZ, USA) was performed on archival paraffin blocks to stain CD68$^+$ macrophages (clone PGM-1, 1:200, Agilent Dako, Santa Clara, CA, USA; pretreatment with Ultra Cell Conditioning Solution

Table 1. Patient characteristics at the time of biopsy

Group	n	Sex (f:m)	Age (yr)	Creatinine (mg/dl)	eGFR (ml/min/1.73 m^2)	CRP (mg/l)	Leukocytes (10^3/μl)
All cases	324	126:198	54 (0–90)	1.98 (0.32–13.06)	33.85 (3.2–171.9)	3.1 (0.1–311.1)	8 (3.1–36.5)
SVV	50	10:23	64.5 (18–89)	2.9 (0.72–9.7)	22 (5–115)	9.92 (0.2–311.1)	11 (4.02–26.07)
IgAN	36	16:34	50 (10–73)	1.3 (0.32–5.25)	57.6 (11.3–135)	2 (0.1–145.8)	7.1 (4.52–21.4)
HTNP	29	11:12	59 (22–83)	2.6 (0.73–5.48)	24.7 (8.4–117.3)	4.05 (0.2–51)	8.7 (4.8–20.2)
MGN	25	09:16	62 (31–78)	1.50 (0.8–4.36)	44.1 (15.4–106.6)	1.5 (0.1–11.6)	7.19 (3.6–13.7)
FSGS	25	12:13	47 (16–82)	1.8 (0.55–10.37)	37 (5.9–127)	2.35 (0.2–37.7)	7.4 (4–36.5)
TMA	23	10:13	43 (19–75)	3.97 (1.2–10.7)	14.7 (5–63)	7.47 (0.2–98)	8.27 (3.55–20)
MCN	23	10:02	54 (14–84)	1.08 (0.71–5.8)	73.2 (10–132.8)	1.4 (0.1–52.8)	7.9 (5.09–15.5)
TIN	21	04:03	48 (14–78)	3.1 (1.1–13.06)	21.7 (3.2–55)	10.65 (0.2–103.5)	6.9 (4–18.7)
DNP	16	08:21	50.5 (27–78)	2.13 (1–9.5)	30.6 (5–77)	3.7 (0.2–69)	8.6 (3.7–15.7)
HTNP/DNP	14	10:11	63 (40–80)	2.2 (0.75–4.3)	31.5 (15–100)	1.48 (0.2–33.1)	8.08 (4.56–20.5)
SLE	12	06:10	41 (18–63)	1.64 (0.64–5.17)	39.05 (9–102.7)	8 (0.1–99.4)	7.3 (3.9–16.4)
TBMS/AS	11	02:12	44 (15–64)	0.95 (0.43–1.8)	89 (32–171.9)	1.8 (0.2–6.3)	7.24 (6.7–12.3)
UTI	9	04:04	50 (12–79)	3.22 (1.65–5.92)	19 (10.5–56.1)	2.6 (1.6–51)	9.2 (4.9–14.2)
Amyloidosis	8	02:07	68 (18–82)	2.44 (0.65–4.37)	24.8 (10–137)	0.54 (0.2–36.4)	8.15 (5.4–11.9)
PIGN	7	05:06	57 (24–82)	1.3 (0.94–5.37)	45.3 (8.8–70)	6.05 (1.5–166)	7.9 (6.7–13)
I/F-GP	7	04:03	65 (36–90)	3.51 (1.19–9.14)	14.5 (7–51)	0.81 (0.1–26.02)	8.5 (5.6–11.1)
Other Diseases	8	03:05	63 (0–81)	3.22 (1.32–4.83)	18.85 (11–62.5)	1.08 (0.5–7.1)	8.26 (3.1–10.8)

CRP, C-reactive protein; DNP, diabetic nephropathy; eGFR, estimated glomerular filtration rate according to Kidney Disease–Improving Global Outcomes; f, female; FSGS, focal segmental glomerulosclerosis; HTNP, hypertensive nephropathy; IgAN, IgA nephritis; I/F-GP, immunotactoid/fibrillary glomerulopathy; m, male; MCN, minimal change glomerulopathy; MGN, membranous glomerulonephritis; PIGN, postinfectious glomerulonephritis; SLE, systemic lupus erythematosus; SVV, small vessel vasculitis/pauci-immune glomerulonephritis; TBMS/AS, thin basement membrane disease/Alport-syndrome; TIN, tubulointerstitial nephritis; TMA, thrombotic microangiopathy; UTI, urinary tract infection; other diseases including: C1q-mesangioproliferative glomerulonephritis (n = 1), C3-mesangioproliferative glomerulonephritis (n = 2), parainfectious mesangiocapillary proliferative glomerulonephritis (n = 1), light-chain nephropathy (n = 1), nicotine-associated nodular glomerulosclerosis (n = 1), lupus-like nephritis (n = 1) and fetofetal transfusion syndrome, associated multiorgan failure, atypical haemolytic uremic syndrome and tubular dysgenesis (n = 1).
HTNP/DNP, HTNP and DNP combined.
Displayed are medians with minimums and maximums in brackets

ULTRA CC1, Ventana Ultra). Subgroups comprising 67 cases of SVV and IgAN were stained manually as follows: Heat Induced Epitope Retrieval was used on rehydrated sections (CD14 and CD163: ethyl-diaminetetraacetate buffer [Zytomed Systems GmbH, Berlin, Germany], pH 9.0, 98 °C, 30 minutes). After peroxidase blocking (3% H_2O_2, 10 minutes), staining was performed by incubation with monoclonal CD14-rabbit-antibody (EPR3656, 1:50) (Cell Marque, Rocklin, CA, USA) and monoclonal CD163-mouse antibody (MRQ-26, 1:1000) (Cell Marque) overnight at 4 °C. After application of the ZytoChem Plus horseradish peroxidase Polymer system (Zytomed Systems GmbH, Berlin, Germany), chromogen visualization with 3,3′-diaminobenzidine (Zytomed) was performed followed by hemalum nuclear staining under standardized conditions. In all staining procedures, negative controls omitting primary antibodies were included. Stained sections were digitalized with a Leica Scanner (Aperio CS2, Leica Microsystems IR GmbH, Wetzlar, Germany) at 40× magnification. Digital analysis of whole-slide images was conducted with the open-source software QuPath[24] by pixel-based precise quantification of positively immunostained areas. The same threshold was applied for all sections, and results were expressed as percentages of positively stained areas of respective regions of interest, renal cortex and medulla (Figure 1, extrarenal tissue was also analyzed, data not shown). Stained and scanned sections were manually reviewed for correctness and artifacts, such as chromogen precipitations or tissue folds, which were excluded from measurements accordingly. The median regions of interest-size of cortex was 5.46 (0.2–17.44) mm^2 and of medulla 2.2 (0.17–8.48) mm^2 (Supplementary Table S1). Densities of whole renal tissue were calculated with the proportional densities of renal cortex and medulla.

Statistical Analysis

IBM SPSS Statistics 26 (IBM, Armonk, NY)[25] was used for statistical analyses. Group comparison was carried out with Kruskal-Wallis test, Mann-Whitney *U* test and Wilcoxon rank sum test. Correlations were analyzed with Spearman rank test. Prediction power was determined using χ^2 test and receiver operating characteristics (ROCs). Renal survival was described with Kaplan-Meyer curve and Log-Rank test. For the latter, macrophages densities were categorized into the groups "low macrophages density" and "high macrophages density," (based on the median CD68 cortical density and ROC-derived cut-

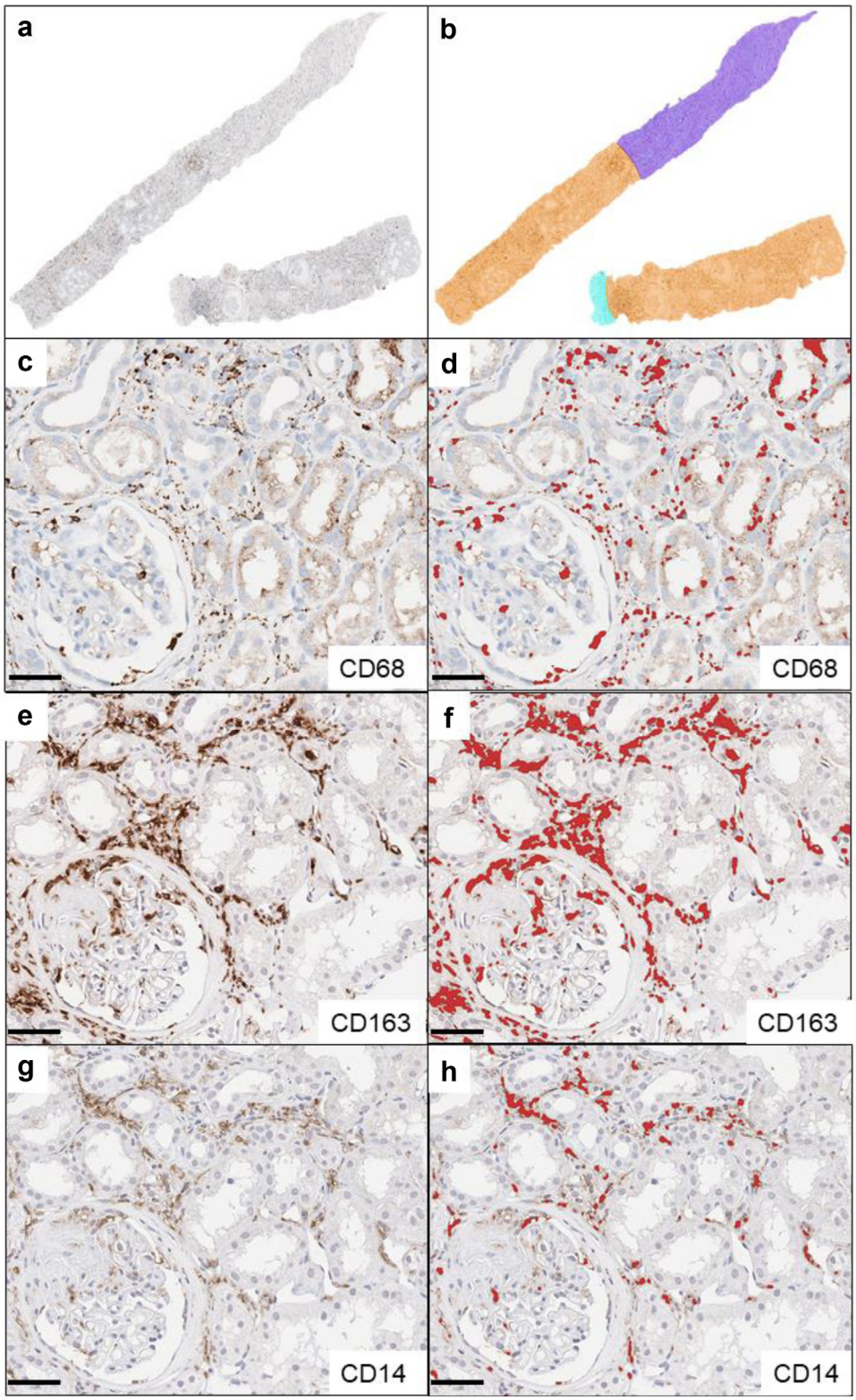

Figure 1. Visualization of histologic and digital methods in a renal biopsy with vasculitis: (a) Whole-slide image of section stained for CD68 (brown). (b) Annotated regions of interests: orange: cortical tissue, dark blue: medullary tissue, light blue: extrarenal tissue. Bar represents 500 μm. (c) Detail of cortical tissue from vasculitis case with CD68-stain for macrophages, (e) CD163-stain for M2-macrophages and (g) CD14-stain for monocytes. Corresponding positive pixel detections shown red; (d): CD68, (f): CD163, (h): CD14. Bars represent 50 μm.

off value). The influence of variables on renal survival was investigated with multivariate Cox regression. Values were presented as median with minimum and maximum, respectively. Significance was assumed at P-value < 0.05, indicated as $^{*}P < 0.05$, $^{**}P < 0.01$ and $^{***}P < 0.001$.

RESULTS

Patient and Clinical Characteristics

Median serum creatinine levels of all 324 patients increased to 1.98 (0.32−13.06) mg/dl, equivalent to a median eGFR of 33.9 (3.2−171.9) ml/min per 1.73 m^2. Systemic inflammation parameters were normal, represented by a median of C-reactive protein of 3.1 (0.1−311.1) mg/l and leukocyte count of 8.0 (3.1−36.5) x 10^3/µl, respectively (Table 1). At biopsy, 23 patients required dialysis treatment; 16 of these patients regained sufficient renal function.

In 50.3% ($n = 163$) of the patients, information about previous renal impairment was available as follows: Acute Kidney Injury Network (AKIN, all stages) was present at the time of biopsy in 25.1% ($n = 41$) of this subcohort; AKIN with underlying CKD (AKIN on CKD) in 21.5% ($n = 35$); and in 53% ($n = 87$) of patients with available prebiopsy data, pre-existing CKD (all stages) was described.

In the subgroup of 158 patients with available follow-up data, a median serum creatinine level of 2.10 (0.55–10.37) mg/dl with a median eGFR of 31.3 (5.0−137.0) ml/min per 1.73 m^2 was measured at time point of biopsy (Supplementary Table S2). At follow-up, patients revealed a median serum creatinine of 1.86 (0.62−11.38) mg/dl with an eGFR of 37.1 (3.6−138.9) ml/min per 1.73m^2, and 26 patients were dependent on permanent dialysis (ESRD; Supplementary Table S2).

Biopsies

The 324 biopsies displayed a median cortex ratio of 80 (5−100)% of total tissue in biopsy, with a median of 16 (2−69) glomeruli (Supplementary Table S3). Medullary tissue was present in 167 biopsies. Global glomerulosclerosis was observed in 236 biopsies affecting a median of 22 (3%−93%) of the glomeruli, and 87 samples presented with segmental glomerulosclerosis with a median of 10% per biopsy (3%−100%). Interstitial fibrosis and tubular atrophy (IF/TA) ranged from 0% to 90% (median 15%) in all biopsies (Supplementary Table S3). The numbers of glomerular crescents (cellular, fibrocellular, and fibrous) as well as necrosis formation are displayed in Supplementary Table S4.

Increased Mononuclear Phagocyte Densities in Renal Disease Compared to Controls

All biopsies with native kidney diseases presented higher $CD68^+$-macrophage densities compared to control samples (whole renal tissue, cortex, and medulla, $P < 0.001$; Table 2, Figure 2a−c). The highest cortical density was observed in systemic lupus erythematosus (SLE) or lupus nephritis and the lowest in thin basement membrane disease and Alport-syndrome. Urinary tract infection presented the highest medullary $CD68^+$ macrophage density and membranous glomerulonephritis presented the lowest medullary $CD68^+$ macrophage density. Cortical and medullary $CD68^+$-macrophage densities correlated with each other across all disease entities ($r = 0.74$, $P < 0.001$).

CKD cases (all stages) showed lower median percentages of $CD68^+$ macrophage infiltration (cortex: 0.8 [0.0−7.4]%; medulla: 0.5 [0.0−1.7]% compared to AKI of all stages (cortex: 1.5 [0.1−9.2]%, $P < 0.001$; medulla: 0.9 [0.1−3.4]%, $P < 0.001$) and acute-on-chronic kidney injury (cortex: 1.7 [0.3−9.9]%, $P < 0.001$; medulla: 1.5 [0.2−2.6]%, $P < 0.001$, Figure 3a and b). These findings were mirrored in whole renal tissue (Figure 3c).

$CD68^+$-Macrophage Densities Correlated With Reduced Kidney Function at Time of Biopsy

$CD68^+$-macrophage densities in cortex and medulla as well as whole renal tissue correlated with the eGFR and risk of ESRD in whole cohort and separate disease entities (Table 3, Figure 4). $CD68^+$ macrophage infiltration in cortex and medulla correlated positively with IF/TA in complete cohort and also in various disease entities (strongest for hypertensive nephropathy: $r = 0.58$, $P < 0.01$; diabetic nephropathy: $r = 0.55$, $P < 0.05$; and combined hypertensive nephropathy/diabetic nephropathy: $r = 0.78$, $P < 0.01$, Supplementary Table S5). No correlation of cortical or medullary $CD68^+$-macrophage densities was observed with serum C-reactive protein, or with blood leukocyte count nor with proteinuria, erythrocyturia and leukocyturia (data not shown). In AKI and CKD, $CD68^+$-macrophage densities correlated weakly with eGFR (AKI: cortex: $n = 41$, $r = -0.31$, $P < 0.05$; medulla: $n = 23$, $r = -0.58$, $P < 0.01$; CKD: cortex: $n = 87$, $r = -0.29$, $P < 0.01$; medulla: $n = 43$, $r = -0.33$, $P < 0.05$, data not shown).

$CD68^+$ Infiltrates Associated With Kidney Disease–Improving Global Outcomes-Stage 5 and a Higher Rate of ERDS at Follow-Up

The time between biopsy and follow-up ranged from 20 to 1675 (median 293.5) days. Initial high $CD68^+$-macrophage densities in cortex and medulla as well as whole renal tissue resulted in a significant decline of renal function until follow-up and predicted ESRD at follow-up (Kidney Disease–Improving Global Outcomes-stage 5; Figure 4, Table 3). Particularly in SVV, high densities of $CD68^+$ macrophage in cortex, medulla, and whole renal tissue in the index biopsies preceded a poor eGFR at follow-up, which was observed in cortex for hypertensive nephropathy and membranous glomerulonephritis, too (Table 3).

The 158 patients with follow-up data were further analyzed according to risk for ESRD as follows: a high cortical $CD68^+$ macrophage density (> median of

Table 2. CD68$^+$-macrophage densities/CD163$^+$-macrophage densities and CD14$^+$-monocyte densities in renal tissues

	Cortex CD68$^+$	Medulla CD68$^+$	Cortex CD163$^+$	Medulla CD163$^+$	Cortex CD14$^+$	Medulla CD14$^+$						
Group	n	Median (%)	n	Median (%)	n	Median (%)	n	Median (%)	n	Median (%)	n	Median (%)
All cases	324	0.88 (0.01–9.86)[a]	167	0.51 (0.01–5.17)[a]	67	2.07 (0.06–26.41)[a]	28	2.29 (0.00–12.08)[b]	67	1.84 (0.00–31.91)[d]	28	1.31 (0.00–23.58)[d]
Controls	8	0.02 (0.00–0.78)	7	0.01 (0.00–0.12)	9	0.37 (0.15–1.649)	9	0.58 (0.09–1.63)	9	0.98 (0.18–1.84)	9	1.29 (0.62–2.94)
SVV	50	1.67 (0.01–9.18)[a]	22	1.07 (0.01-2.51)[a]	36	4.01 (0.06–26.41)[a]	12	4.03 (0.34–12.08)[a]	36	2.00 (0.00–15.12)[d]	12	1.98 (0.04–23.58)[d]
IgAN	36	0.56 (0.09–2.90)[a]	19	0.31 (0.09–2.86)[a]	31	1.00 (0.09–6.23)[c]	16	1.61 (0.00–4.18)[d]	31	1.37 (0.00–31.91)[d]	16	0.944 (0.00–15.91)[d]
HTNP	29	0.87 (0.07–2.55)[a]	16	0.45 (0.07–1.47)[a]	n.e.							
MGN	25	0.50 (0.06–2.75)[b]	10	0.09 (0.01–1.52)[d]								
FSGS	25	0.60 (0.07–3.74)[a]	12	0.41 (0.03–5.12)[b]								
TMA	23	1.37 (0.31–3.35)[a]	12	0.66 (0.21–1.94)[a]								
MCN	23	0.38 (0.03–6.37)[b]	12	0.19 (0.12–1.69)[a]								
TIN	21	1.3 (0.11–5.99)[a]	11	0.95 (0.12–4.38)[a]								
DNP	16	0.83 (0.18–5.43)[a]	10	0.52 (0.12–5.17)[a]								
HTNP/DNP	14	0.74 (0.01–2.73)[b]	7	0.74 (0.40–2.60)[b]								
SLE	12	1.98 (0.71–3.54)[a]	7	0.73 (0.31–2.38)[b]								
TBMS/AS	11	0.18 (0.01–1.94)[c]	8	0.21 (0.10–0.69)[b]								
UTI	9	1.43 (0.48–5.87)[a]	4	2.05 (0.73–2.60)[b]								
Amyloidosis	8	1.08 (0.62–2.86)[b]	5	0.27 (0.10–1.25)[c]								
PIGN	7	1.11 (0.33–1.82)[b]	5	0.88 (0.25–1.98)[b]								
I / F-GP	7	0.71 (0.26–1.31)[b]	3	0.17 (0.11–0.50)[d]								
Other diseases	8	1.83 (0.78–9.86)[a]	4	0.85 (0.48–2.79)[b]								

DNP, diabetic nephropathy; FSGS, focal segmental glomerulosclerosis; HTNP, hypertensive nephropathy; IgAN, IgA nephritis; I/F-GP, immunotactoid/fibrillary glomerulopathy; MCN, minimal change glomerulopathy; MGN, membranous glomerulonephritis; n.e, not evaluated; PIGN, postinfectious glomerulonephritis; SVV, small vessel vasculitis/pauci-immune glomerulonephritis; SLE, systemic lupus erythematosus; TBMS/AS, thin basement membrane disease/Alport-syndrome; TIN, tubulointerstitial nephritis; TMA, thrombotic microangiopathy; UTI, ascending infection/urinary tract infection.
HTNP/DNP, HTNP and DNP combined.
CD68$^+$-macrophage densities/CD163$^+$-macrophage densities and CD14$^+$-monocyte densities (% area) of renal cortex and medulla presented as median (minimum–maximum).
Significant differences compared to controls (Mann-Whitney U test) are displayed
[a] $P < 0.05$.
[b] $P < 0.01$.
[c] $P < 0.001$.
[d] Not significant.
Data of CD163 and CD14 were only collected in SVV and IgAN (n.e. or n < 10).

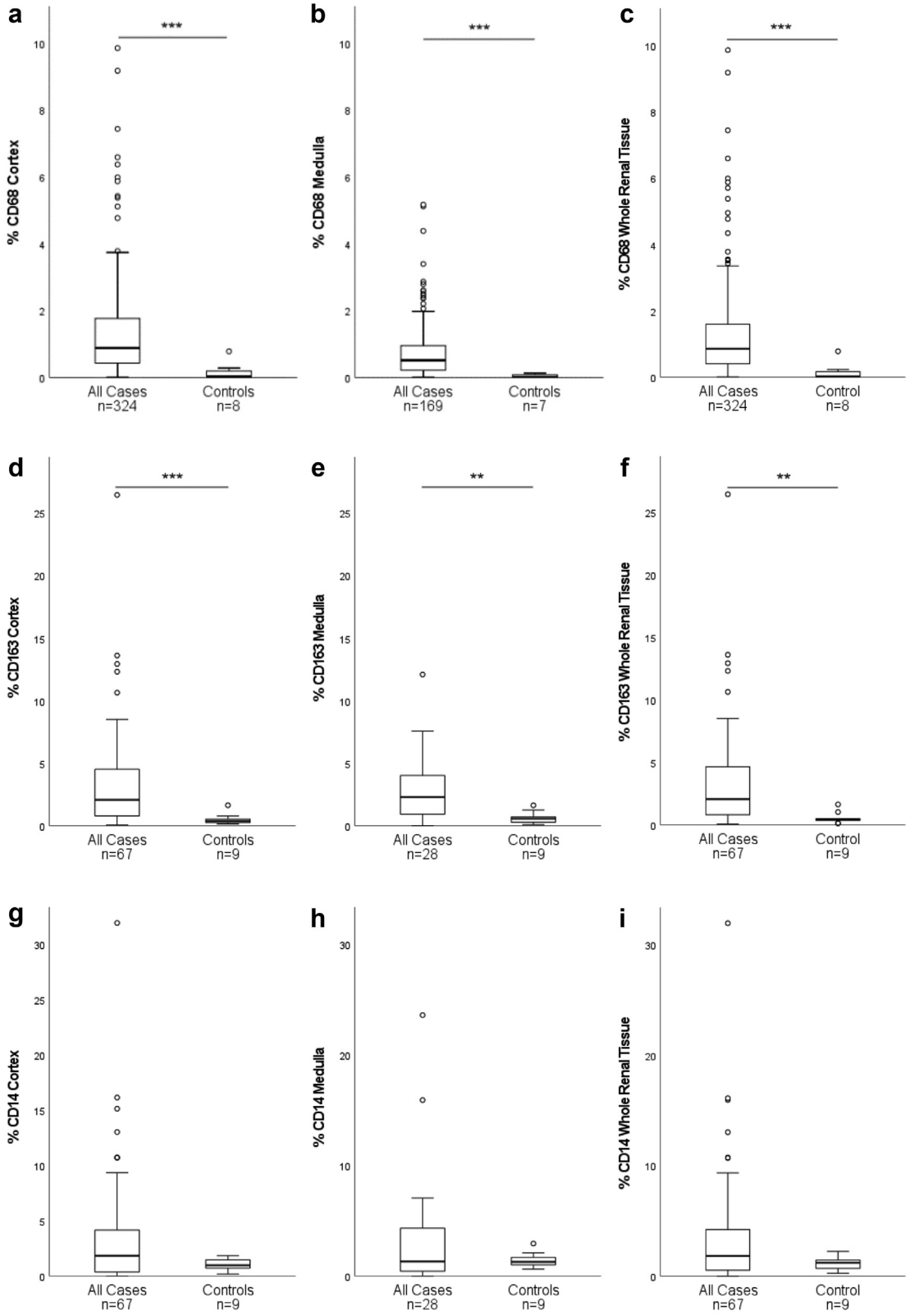

Figure 2. Macrophage and monocyte densities (% area) in all diseased cases compared to controls. $CD68^{+}$-densities in cortex (a), medulla (b), whole renal tissue (c) and $CD163^{+}$-densities in cortex (d), medulla (e) and whole renal tissue (f) are higher in native kidney diseases (cases) compared to normal kidneys (controls). $CD14^{+}$-densities in cortex (g), medulla (h) and whole renal tissue (i) do not differ between cases and controls. (*$P < 0.05$, **$P < 0.01$, ***$P < 0.001$; box: 1. -3. quartile, low whisker: 1. quartile – 1.5 × interquartile range, high whisker: 3. quartile + 1.5 × interquartile range; °: outlier).

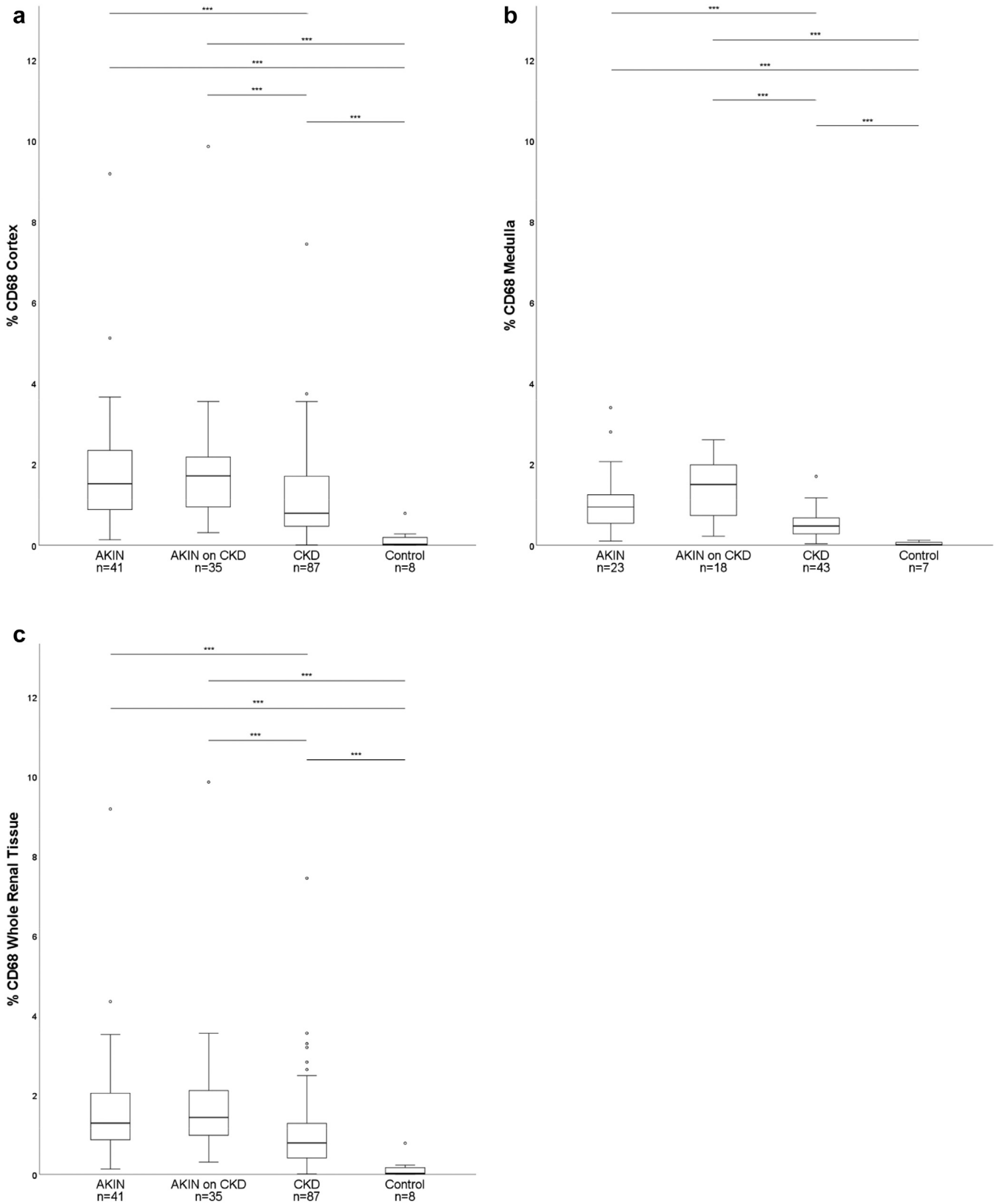

Figure 3. Macrophage densities (% CD68-immunostained area) in renal cortex (a), medulla (b) and whole renal tissue (c) in acute kidney injury of all stages according to RIFLE-criteria (AKIN), AKIN with an underlying chronic kidney disease (AKIN on CKD), and chronic kidney disease of all stages according to KDIGO (CKD), compared to controls with normal renal tissue. Boxes show the medians with quartile ranges, whiskers display 1.5 × interquartile range of the 1. and 3. quartile. (*** $P < 0.001$; °outlier).

Table 3. Correlations and predictive values of $CD68^+$-densities at biopsy and follow-up

$CD68^+$-density			At biopsy						At follow-up					
			n	Cortex	n	Medulla	n	Whole Tissue	n	Cortex	n	Medulla	n	Whole Tissue
Spearman's r	All cases	Creatinine	323	0.512[a]	166	0.59[a]	323	0.54[a]	156	0.412[a]	81	0.389[a]	156	0.422[a]
		eGFR	324	−0.509[a]	167	−0.596[a]	324	−0.532[a]	158	−0.409[a]	83	−0.343[b]	158	−0.413[a]
	SVV	eGFR	50	−0.534[a]	22	−0.662[b]	50	−0.541[a]	39	−0.434[b]	18	−0.507[c]	39	−0.465[b]
	IgAN	eGFR	36	−0.392[c]	19	−0.292[d]	36	−0.447[b]	15	−0.275[d]		n.e.	15	−0.271[d]
	HTNP	eGFR	29	−0.439[c]	16	−0.668[b]	29	−0.481[b]	11	−0.77[b]		n.e.	11	−0.806[b]
	MGN	eGFR	25	−0.701[a]	10	−0.733[c]	25	−0.716[a]	16	−0.576[b]		n.e.	16	−0.571[c]
	FSGS	eGFR	25	−0.634[b]	12	−0.666[c]	25	−0.696[a]		n.e.		n.e.		n.e.
χ^2	All cases	KDIGO	324	64.748[a]	167	59.780[a]	324	73.62[a]	158	19.743[b]		n.e.	158	21.775[a]

eGFR, estimated glomerular filtration rate; FSGS, focal segmental glomerulosclerosis; HTNP, hypertensive nephropathy; IgAN, IgA nephritis; KDIGO, Kidney Disease–Improving Global Outcomes; MGN, membranous glomerulonephritis; n.e., not evaluated; SVV, small vessel vasculitis.
[a]$P < 0.001$.
[b]$P < 0.01$.
[c]$P < 0.05$.
[d]Not significant.
χ^2 analysis included all KDIGO stages. Missing values (n.e.) were either not measured or the analyzed group was $n < 10$. serum creatinine: mg/dl, eGFR: ml/min/1.73 m^2.
Correlations (Spearman's r) and predictive values (χ^2) of $CD68^+$-densities in cortex, medulla, and whole renal tissue with or for renal function, respectively (estimated glomerular filtration rate; KDIGO; ml/min/1.73 m^2) at biopsy and at follow-up.

0.875%; Figure 5a and b) in the initial biopsy predicted a higher risk of ESRD at follow-up in whole cohort and subcohort with follow-up data >365 days ($P < 0.05$). Kaplan-Meier curves, based on ROC-derived separation of cohorts (< / > 0.7998%), confirmed this finding (Figure 5c and d). When follow-up data >182 or >274 days were included, respectively, Kaplan-Meier curves based on ROC-derived cohort separation (0.7998%)

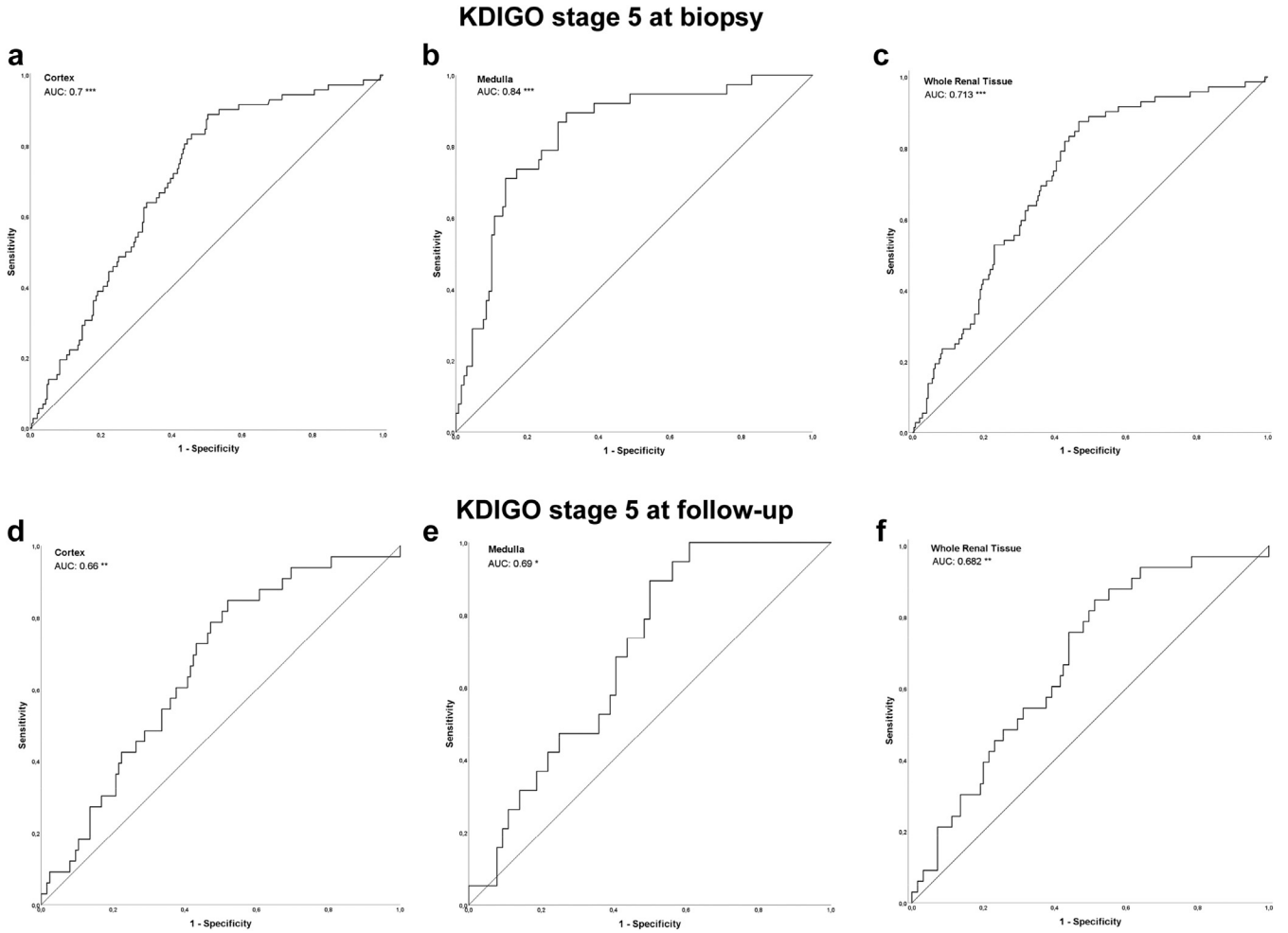

Figure 4. Receiver operating characteristics (bold curve) with AUC-values of severe impairment of renal function (KDIGO stage 5) and $CD68^+$-macrophage densities at biopsy in cortex (a; n = 324), medulla (b; n = 167) and whole renal tissue (c; n = 324), as well as at follow-up (complete cohort) in cortex (d; n = 158), medulla (e; n = 83) and whole renal tissue (f; n = 158). The fair curve is the reference AUC = 0.5 in a–f. (* $P < 0.05$, ** $P < 0.01$, *** $P < 0.001$). AUC, area under the curve.

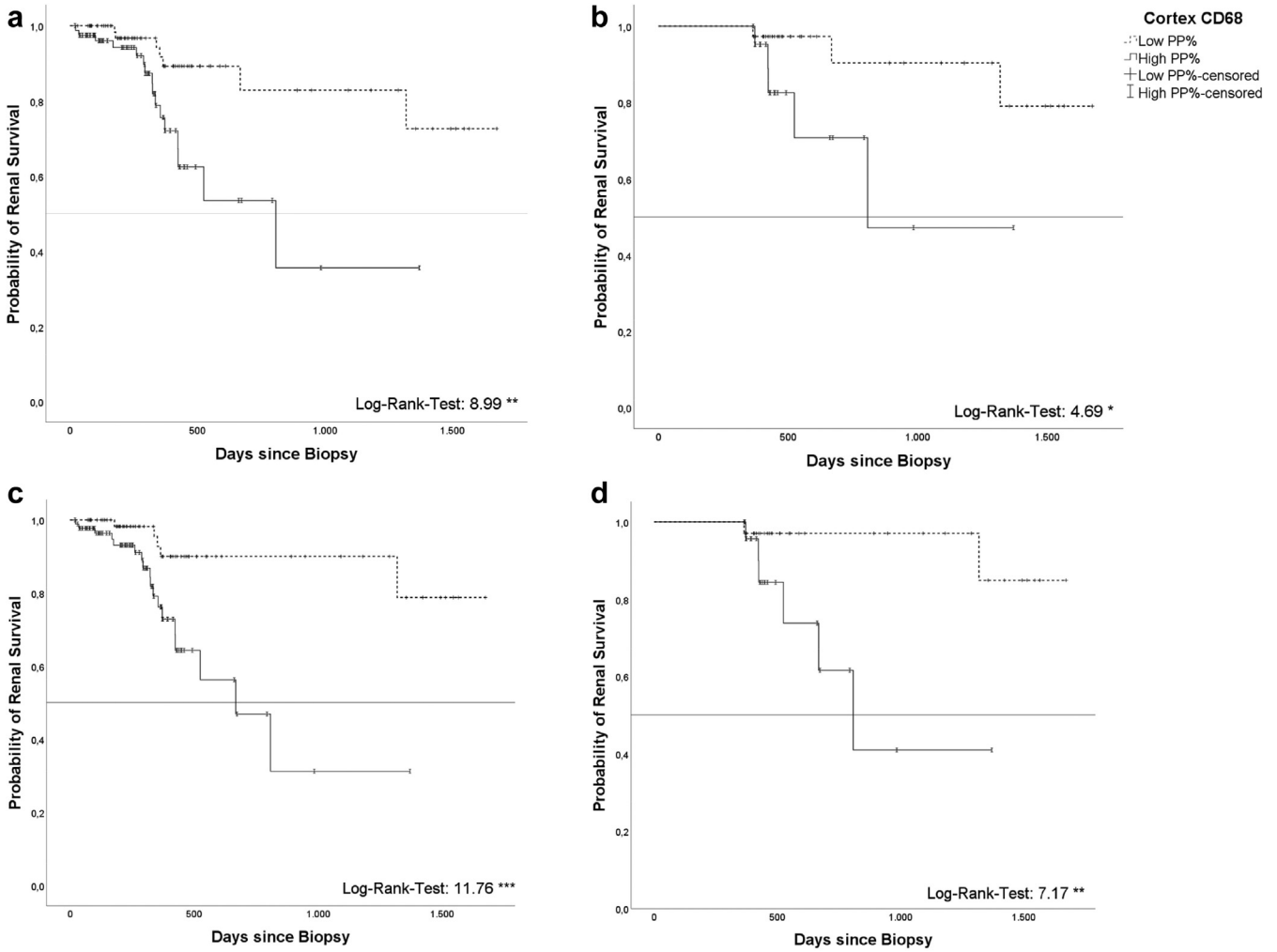

Figure 5. Kaplan-Meyer curve showing cumulative kidney survival at follow-up for entire follow-up cohort (a; n = 158) comparing low (< median; n = 76) and high (> median; n = 82) cortical CD68$^+$ densities (log rank 8.989 **) and for subcohort with outcome data >365 days (b; n = 60, < median n = 37; > median n = 23), respectively. c and d depict the cumulative kidney survival using a ROC-derived (receiver operating characteristics derived) separation value (c: entire cohort, n = 158, < ROC-derived separation value n = 68, > ROC-derived separation value n = 90; d: subcohort with outcome data >365 days, n = 60, < ROC-derived separation value n = 34, > ROC-derived separation value n = 26). (* P < 0.05, ** P < 0.01, *** P < 0.001). Median of 0.875% and ROC-derived separation value of 0.7998% were calculated in whole study cohort (n = 324). ROC, receiver operating characteristics.

showed comparable results regarding the risk of ESRD with high densities of cortical CD68 positive cells (Supplementary Figures S1 and S2).

Multivariable Cox regression revealed a 4-fold higher risk of ESRD when macrophage density was above median (hazard ratio = 3.911, $P < 0.05$), whereas %IF/TA had minimal effect (hazard ratio = 1.032, $P < 0.001$) on ESRD (Table 4). Patient age, global sclerosis of glomeruli, presentation (AKIN, AKIN on CKD, or CKD) or sex had no significant effect (Table 4).

IgA and SVV Subcohorts: CD68$^+$ Macrophages, CD163$^+$ Macrophages and CD14$^+$-Monocytes

Subtyping of macrophages in all 67 biopsies showed higher CD163$^+$-macrophage densities compared to controls (Table 2, Figure 2d–f). CD14$^+$-monocyte densities in cortex, medulla and whole renal tissue did not differ from controls (Table 2, Figure 2g–i). The CD163$^+$-macrophage densities correlated with CD68$^+$-macrophage densities in cortex, medulla and whole renal tissue and inversely with eGFR at the time point of biopsy (Table 5). At follow-up, high initial CD163$^+$-macrophage densities associated with reduced eGFR (Table 5). CD14$^+$-monocyte density correlated with CD68$^+$ macrophage density in cortex (cortex: $r = 0.39$, $P < 0.01$). CD14$^+$-monocyte densities did not associate with renal function at time of biopsy or at follow-up (Table 5) or with IF/TA (Supplementary Table S5). When we compared areas of high CD68$^+$-macrophage densities with areas of IF/TA in biopsies with diagnosed SVV, there was no consistent association, especially fibrotic areas did not show higher densities of macrophages (Supplementary Figure S3).

Patients with SVV were further grouped according to antibody status and disease activity as follows:

Table 4. Hazard ratios of variables at biopsy from univariable and multivariable Cox regression analysis

	Univariable analysis			Multivariable analysis		
	HR	CI 95%	*P*-value	HR	CI 95%	*P*-value
Age at Biopsy (yr)	1.013	0.991 1.036	0.240			
Gender (female)	1.901	0.878 4.114	0.103			
CD68 MΦ Cortex (high)	5.913	2.159 16.196	0.001	3.911	1.342 11.401	0.012
KDIGO stage 5 at biopsy	3.562	1.645 7.714	0.001			
% global glomerulosclerosis	1.105	1.042 1.173	0.001			
% IF/TA	1.039	1.024 1.054	< 0.001	1.032	1.016 1.048	< 0.001

HR, hazard ratio; IF/TA, interstitial fibrosis and tubular atrophy; KDIGO, Kidney Disease–Improving Global Outcomes.
95% confidence intervals are given with the upper and lower boundaries. ROC-curve (receiver operating characteristics) derived groups of high/low CD68 MΦ-densities (% area) of renal cortex.

cortical $CD68^+$- and $CD163^+$-macrophage densities were measured highest in ANCA-negative vasculitis, whereas biopsies with nonactive vasculitis presented the highest cortical $CD14^+$-monocyte density (Supplementary Table S6). In cytoplasmic anti-neutrophil cytoplasmic antibody ($cANCA^+$)-vasculitis, a strong inverse correlation occurred between eGFR at biopsy and $CD68^+$-macrophage densities in cortex (r = -0.78, $P < 0.001$) and medulla ($r = -0.65$, $P < 0.05$) as well as with cortical $CD163^+$-macrophage density at biopsy ($r = -0.75$, $P < 0.001$) and at follow-up ($r = -0.68$, $P < 0.01$, Supplementary Figure S4).

Supplementary Table S7 depicts the distribution of Berden score[21] and Brix score[22] in biopsies with SVV diagnosis. Berden score was used for histopathologic classification of biopsies with SVV. The eGFR at the time of biopsy or at follow-up did not differ significantly between the classes. $CD68^+$-macrophage densities in whole renal tissue were significantly higher in crescentic class compared to mixed class ($P < 0.05$) and cortical CD68 macrophage density was also higher in crescentic class than in focal class and mixed class, respectively ($P < 0.01$). Brix renal risk score for ANCA-associated glomerulonephritis identified 25 cases with low risk for ESRD, 20 cases with an intermediate risk and a high risk for ESRD was stated in 5 cases. The predicted renal risk correlated inversely with eGFR at the time of biopsy ($r = -0.86$, $P < 0.001$) and at the time of follow-up ($r = -0.64$, $P < 0.001$). $CD68^+$-macrophage densities in cortex, medulla and whole renal tissue as well as $CD163^+$-macrophage densities in cortex and whole renal tissue correlated with the predicted renal risk, too (CD68 cortex: $r = 0.41$, $P < 0.01$; CD68 medulla: $r = 0.67$, $P < 0.01$; CD68 whole renal tissue: $r = 0.44$, $P < 0.01$; CD163 cortex: $r = 0.46$, $P < 0.01$, CD163 whole renal tissue: $r = 0.47$, $P < 0.01$). Global glomerular sclerosis

Table 5. Correlations of $CD163^+$ and $CD14^+$ densities at biopsy and follow-up

			Both subgroups				Subgroups separately			
			Creatinine		eGFR		eGFR			
Spearman's *r*			n		n		n	SVV	n	IgAN
$CD163^+$	At biopsy	Cortex	67	0.677[a]	67	−0.705[a]	36	−0.577[a]	31	−0.468[b]
		Medulla	28	0.707[a]	28	−0.73[a]	12	−0.413[d]	16	−0.582[c]
		Whole tissue	67	0.687[a]	67	0.718[a]	36	−0.588[a]	31	−0.502[b]
	At follow-up	Cortex	46	0.431[b]	46	−0.458[b]	36	−0.512[b]	10	−0.042[d]
		Medulla	18	0.418[c]	18	−0.501[c]	12	−0.399[d]		n.e.
		Whole tissue	46	0.453[b]	46	−0.48[a]	36	−0.531[a]	10	−0.164[d]
$CD14^+$	At biopsy	Cortex	67	0.157[d]	67	−0.172[d]	36	−0.241[d]	31	−0.201[d]
		Medulla	28	0.052[d]	28	−0.094[d]	12	−0.084[d]	16	0.315[d]
		Whole tissue	67	0.144[d]	67	−0.16[d]	36	−0.234[d]	31	0.018[d]
	At follow-up	Cortex	46	0.189[d]	46	−0.162[d]	36	−0.276[d]	10	−0.164[d]
		Medulla	18	−0.075[d]	18	−0.110[d]	12	−0.084[d]		n.e.
		Whole tissue	46	0.169[d]	46	−0.143[d]	36	−0.258[d]	10	0.212[d]

eGFR, estimated glomerular filtration rate; IgAN, IgA nephritis; n.e., not evaluated; SVV, small vessel vasculitis.
Subgroups SVV and IgAN (together and separately): correlations (Spearmans' *r*) of $CD163^+$-densities/$CD14^+$-densities with serum creatinine (mg/dl) and KDIGO; ml/min/1.73 m^2), respectively, in cortex, medulla, and whole renal tissue at biopsy and at follow-up.
[a] $P < 0.001$.
[b] $P < 0.01$.
[c] $P < 0.05$.
[d] Not significant.
n.e. or n < 10.

was higher in cases with a high renal risk compared to cases with low or intermediate renal risk ($P < 0.05$).

In IgAN, IF/TA correlated positively with cortical $CD163^+$-macrophage densities (Supplementary Table S5). Regarding official classifications, the distribution of findings in IgA nephropathy according to the Oxford classification is shown in Supplementary Table S8.[23] The eGFR at biopsy correlated with $CD68^+$-macrophage densities and $CD163^+$-macrophage densities (Table 3, cortex: $r = -0.47$, $P < 0.01$; medulla: $r = -0.58$, $P < 0.05$), but not at follow-up. Regarding MEST-C-criteria (M: mesangial hypercellularity, E: endocapillary hypercellularity, S: segmental glomerulosclerosis, T: IF/TA, C: crescents), eGFR at biopsy was lower in biopsies with crescent formation compared to those without crescents ($P < 0.01$). $CD68^+$-macrophage densities in cortex and whole renal tissue were higher in cases with T-score 1 (IF/TA $> 25\%$) compared to T-score 0 ($P < 0.05$).

Medication

In a subcohort of 106 patients, data on medication was available (Supplementary Table S9). Depending on the disease entity, up to one-third of all patients received an immunosuppressive therapy because of the biopsy result, often with more than 1 immunosuppressive drug. A considerable proportion of patients had received immunosuppressive treatments before or at the time of the index biopsy, indicating patients with a rather chronic course of their disease. Because of the small number of cases for each disease entity, it was not possible to compare treated patients with patients without treatment or to analyze different immunosuppressive drug combinations regarding outcome. Over all disease entities, immunosuppressive treatment was associated with a nonsignificant increase in eGFR at follow-up whereas patients without treatment had a decrease (median of +0.011 vs. −0.0177 ml/min daily; $P = 0.122$). Macrophage densities were not different between treated patients and those without treatment (0.78 vs. 0.91%, $P = 0.77$).

DISCUSSION

In the present study, we precisely quantified the prevalence of macrophages and monocytes using digital histomorphology on whole-slide images in a retrospective cross-sectional cohort of native kidney diseases and linked them to renal function and clinical outcome, including need of permanent dialysis. The cross-sectional nonselective character of our study resulted in a representative random sample of native kidney diseases typically diagnosed in nephropathology units. We observed higher macrophage densities in immunologic and nonimmunologic renal diseases compared to normal kidney tissue. Our results reveal a negative correlation between macrophage densities in renal cortex and medulla as well as whole renal tissue with renal function at time of initial biopsy and at follow-up, which persisted if follow-up data were analyzed for later time points. Moreover, high densities (based on median or ROC-derived cut-off for CD68+ area within cortex) of macrophages coincided with increased risk for ESRD. This indicates a participation of macrophages in progressive tissue damage during renal diseases independent of the underlying cause.

In general, cell counting of macrophages is difficult because these cells are characterized by variable shape if compared to more round appearing lymphocytes.[26] Therefore, we decided to measure immunostained areas. The measured values of CD163 positive cells (M2 macrophage) were higher compared to CD68 (all macrophage), which most probably is based on a technical aspect. Direct comparison of both markers is problematic, because CD163 detects a cell surface glycoprotein, which might result in far more extensive labeled area compared to CD68/PG-M1 binding to a lysosomal protein.[27–29] There is no specific marker for M1 macrophage, which works in formalin-fixed paraffin-embedded tissues.

The densities measured coincided with severity and acuity of inflammation, reflected by the highest values for SLE and SVV in cortex and for urinary tract infection in medulla. Similarly, lower densities were present in CKD compared with acute and acute-on-chronic renal disease. Moreover, densities of $CD68^+$ (all macrophages) and $CD163^+$-cells but not $CD14^+$ cells (monocytes), correlated with severity of function impairment at biopsy (at the time point of hospital admission). The observed negative correlation with renal function was strong in SVV and membranous glomerulonephritis, and for both diseases persisted at follow-up, indicating a direct role of macrophages in renal damage.

Our findings are consistent with previously published data as follows: first, the correlation of macrophage infiltration with the degree of injury in human AKI;[30] and second, after ischemia reperfusion injury in human renal tissue, where $CD163^+$-macrophage densities predicted renal function loss.[31] In a murine ANCA-associated vasculitis model, a direct role of monocytes and macrophages was shown in areas of glomerular necrosis and crescent formation,[32] and soluble CD163 (sCD163) was reported as a urinary disease marker in rats with renal vasculitis.[33] In humans with biopsy-proven renal vasculitis, urinary sCD163 paralleled disease activity[34–36] and $CD163^+$ macrophages colocalized with necrotic glomerular lesions.[37] A similar correlation of $CD163^+$ macrophages and urinary

sCD163 with disease activity was reported in SLE.[38–40] Further, the quantity of glomerular CD68$^+$ cells was used as a surrogate marker for endocapillary hypercellularity in SLE.[41] This also applies in IgAN, and in addition, glomerular macrophages predicted functional decline and interstitial CD68$^+$ macrophages coincided with chronic damage.[42,43] Interstitial CD163$^+$ macrophages indicated crescent formation with associated chronic renal failure in IgAN and purpura Schönlein-Henoch.[44,45] These data are in line with the strong negative correlation of CD68$^+$- and CD163$^+$-macrophage densities with renal function in our study.[46]

No definite conclusions were possible regarding immunosuppressive treatments and their efficacy. Treatment data were available only in few cases and therapeutic regimes were heterogeneous in these patients. In addition, treatment bias (e.g., because of disease severity) and different treatment standards has to be taken into account. For example, all patients with SLE received treatment whereas only one-third of patients with IgAN was treated. However, none of the applied compounds are known to serve as direct macrophage targeted therapy. Most patients received steroids, which can have both activating or suppressive effect on macrophages[47,48] and monocytes, dependent on steroid concentration and macrophage/monocyte phenotype and activation state, which limits interpretation of our treatment data.

Indicated immunologic therapies in native kidney diseases definitely play a beneficial role in long-term renal function, but macrophage might at least partly be missed by application of standard regimes.[46] One study published a trend toward a better graft function in renal transplantation by inhibition of macrophages using ibandronate medication, but without direct analysis of macrophage density in renal tissue.[49,50] Several (clinical) studies, mainly in oncology, target macrophages directly by depletion or reducing survival, repolarization or reshaping of macrophages, or suppressing macrophage recruitment or blocking monocyte infiltration using small molecules, antibodies, or chimeric antigen receptor T-cell therapy, which are all promising agents also for nontumorous inflammatory diseases.[48]

Elevated blood counts of monocytes have been associated with risk for CKD and progression to ESRD.[51,52] Our data on renal CD14$^+$ cells do not point to this direction, but blood monocytes may not necessarily reflect local CD14 presence in renal tissue because of differentiation into polarized CAR (CD68+) with loss of CD14 epitopes after migration from blood into the tissue.[53]

A negative correlation of macrophage densities with renal function and an increased risk of reduced kidney survival by high cortical CD68$^+$-macrophage densities was established in the present study. In our previous work using protocol biopsies at a defined early time point following renal transplantation, we were able to show a significant interrelationship between macrophage infiltration and renal function[54]: In early (6 weeks after transplantation) protocol biopsies, the cortical CD68$^+$-macrophage density was associated with patient and graft survival as well as delayed graft function. Similar to our present findings, macrophage density was predictive for function loss and future graft function.[54] Global sclerosis of glomeruli and IF/TA have been accepted markers for long-term renal function loss, but are not predictive in the true sense, because they represent irreversible loss of functional tissue. Macrophages are known contributors to tissue fibrosis. In the present study we did not observe consistently higher macrophage densities in fibrotic renal areas. Our finding that AKI and AKI-on-CKD cases showed higher macrophage densities compared to CKD without AKI might point toward a contribution of macrophages to active inflammation and developing fibrosis but evasion if fibrosis is fully established. This is supported by other publications.[55,56] A direct causative relation between macrophage density and fibrosis cannot be drawn from our data; however, multivariable Cox regression showed a 4-fold higher ESRD risk for high macrophage density (above median), whereas IF/TA or global sclerosis of glomeruli had almost no effect.

Renal cortex and medulla were evaluated separately because inflammation and immune cell infiltration is often more severe in medulla than in cortex. Because of the different micromilieu (e.g., renal osmolyte concentrations, chemokine concentration) in these 2 kidney compartments, the distribution (more medullary than cortical macrophages in healthy kidneys) and the phenotypes of mononuclear phagocytes differ significantly, which we described before in renal grafts and native kidneys.[15,57]

Our findings show that innovative predictive data can be generated by increasing precision and objectivity using digitally-based morphologic analyses and improving published quantitative or semiquantitative approaches.[58–60] Actually, advanced digital approaches using deep learning or convolutional neuronal networks for analyzing morphologic parameters in renal tissues are under development, which might further increase precision.[61–63]

The present study, to the best of our knowledge, is the first to show an association of macrophage densities with renal function and risk for ESRD in a disease

overarching cohort of native kidney diseases. Our consistent results are strengthened by the cross-sectional study design (multicentric character, heterogeneous cohort, stable findings independent of patient age, sex, biopsy time point within course of disease or underlying pathophysiology). Limitations might be size of the patient cohorts and subcohorts, and limited specific macrophage subtype markers for human paraffin-embedded tissues.

In summary, this study demonstrates strong evidence of a detrimental role of macrophages in various human kidney diseases and their potential for risk stratification. Further studies are needed to determine whether and to which extent macrophages and their specific subtypes have a bystander or independent role in renal injury. Macrophages act in a disease spanning manner and might be a promising target for future treatment strategies.

DISCLOSURE

All the authors declared no competing interests.

ACKNOWLEDGMENTS

The authors thank Mahtab Taleb-Naghsh and Edda Christians for excellent technical assistance.

Funding

JS and JHB received funding from German Federal Ministry of Education and Research (BMBF No. 13GW0399B).

AUTHORS CONTRIBUTIONS

JS and JHB conceived and designed the research; KS, HT, AW, AKu, UK, SD, JTK, WG and HH collected renal samples and provided clinical data; JHB and AKh revaluated renal tissues; JS performed experiments; MBP measured cellular densities, MBP, JS, WG, IS and JHB analyzed data, interpreted results, prepared figures, and drafted the manuscript; MBP, JS, JHB, KS, AKh, HT, AW, AKu, UK, SD, JTK, IS, WG, and HH revised and approved final version of the manuscript.

SUPPLEMENTARY MATERIAL

Supplementary File (PDF)

Figure S1. Kaplan-Meier curves in cohorts with follow-up data >182 and >274 days.

Figure S2. ROC analysis of CD68+ densities and KDIGO stage 5 with different times of follow-up.

Figure S3. Macrophages and fibrosis in native renal biopsies.

Figure S4. Correlations of CD68 and CD163 with eGFR in cANCA^{+}-vasculitis.

Table S1. Size (median) of regions of interest (ROI, cortex and medulla).

Table S2. Characteristics of patients with available follow-up data.

Table S3. Morphologic characteristics of native renal biopsies.

Table S4. Crescent Formation per biopsy.

Table S5. Correlations of immune cell densities with interstitial fibrosis and tubular atrophy (IF/TA).

Table S6. Clinical characteristics of patients with small vessel vasculitis and macrophage/monocyte densities.

Table S7. Berden Score and Brix-Score in biopsies with small vessel vasculitis.

Table S8. Oxford Classification of IgA nephritis.

Table S9. Immunosuppressive therapies before, at, and after renal biopsy, and at follow-up.

REFERENCES

1. Duffield JS. Cellular and molecular mechanisms in kidney fibrosis. *J Clin Invest*. 2014;124:2299–2306. https://doi.org/10.1172/JCI72267
2. Netea MG, Balkwill F, Chonchol M, et al. A guiding map for inflammation. *Nat Immunol*. 2017;18:826–831. https://doi.org/10.1038/ni.3790
3. Gurtner GC, Werner S, Barrandon Y, Longaker MT. Wound repair and regeneration. *Nature*. 2008;453:314–321. https://doi.org/10.1038/nature07039
4. Chawla LS, Eggers PW, Star RA, Kimmel PL. Acute kidney injury and chronic kidney disease as interconnected syndromes. *N Engl J Med*. 2014;371:58–66. https://doi.org/10.1056/NEJMra1214243
5. Murray PJ, Wynn TA. Protective and pathogenic functions of macrophage subsets. *Nat Rev Immunol*. 2011;11:723–737. https://doi.org/10.1038/nri3073
6. Banerjee A, Stevenaert F, Pande K, et al. Modulation of paired immunoglobulin-like type 2 receptor signaling alters the host response to Staphylococcus aureus-induced pneumonia. *Infect Immun*. 2010;78:1353–1363. https://doi.org/10.1128/IAI.00969-09
7. Dai H, Lan P, Zhao D, et al. PIRs mediate innate myeloid cell memory to nonself MHC molecules. *Science*. 2020;368:1122–1127. https://doi.org/10.1126/science.aax4040
8. Mills CD, Kincaid K, Alt JM, et al. M-1/M-2 macrophages and the Th1/Th2 paradigm. *J Immunol*. 2000;164:6166–6173. https://doi.org/10.4049/jimmunol.164.12.6166
9. Murray PJ, Allen JE, Biswas SK, et al. Macrophage activation and polarization: nomenclature and experimental guidelines. *Immunity*. 2014;41:14–20. https://doi.org/10.1016/j.immuni.2014.06.008
10. Schroder K, Irvine KM, Taylor MS, et al. Conservation and divergence in toll-like receptor 4-regulated gene expression in primary human versus mouse macrophages. *Proc Natl Acad Sci U S A*. 2012;109:E944–E953. https://doi.org/10.1073/pnas.1110156109
11. Reynolds G, Haniffa M. Human and mouse mononuclear phagocyte networks: a tale of two species? *Front Immunol*. 2015;6:330. https://doi.org/10.3389/fimmu.2015.00330

12. Martinez FO, Gordon S. The M1 and M2 paradigm of macrophage activation: time for reassessment. *F1000 Prime Rep*. 2014;6:13. https://doi.org/10.12703/P6-13
13. Tang PM, Nikolic-Paterson DJ, Lan H. Macrophages: versatile players in renal inflammation and fibrosis. *Nat Rev Nephrol*. 2019;15:144–158. https://doi.org/10.1038/s41581-019-0110-2
14. Xue J, Schmidt SV, Sander J, et al. Transcriptome-based network analysis reveals a spectrum model of human macrophage activation. *Immunity*. 2014;40:274–288. https://doi.org/10.1016/j.immuni.2014.01.006
15. Casper J, Schmitz J, Bräsen JH, et al. Renal transplant recipients receiving loop diuretic therapy have increased urinary tract infection rate and altered medullary macrophage polarization marker expression. *Kidney Int*. 2018;94:993–1001. https://doi.org/10.1016/j.kint.2018.06.029
16. Smith SR, Schaaf K, Rajabalee N, et al. The phosphatase PPM1A controls monocyte-to-macrophage differentiation. *Sci Rep*. 2018;8:902. https://doi.org/10.1038/s41598-017-18832-7
17. Shi C, Pamer EG. Monocyte recruitment during infection and inflammation. *Nat Rev Immunol*. 2011;11:762–774. https://doi.org/10.1038/nri3070
18. Levey AS, Stevens LA, Schmid CH, et al. A new equation to estimate glomerular filtration rate. *Ann Intern Med*. 2009;150:604–612. https://doi.org/10.7326/0003-4819-150-9-200905050-00006
19. Stevens PE, Levin A, Kidney Disease, Improving Global Outcomes Chronic Kidney Disease Guideline Development Work Group Members. Evaluation and management of chronic kidney disease: synopsis of the kidney disease: improving global outcomes 2012 clinical practice guideline. *Ann Intern Med*. 2013;158:825–830. https://doi.org/10.7326/0003-4819-158-11-201306040-00007
20. Venkataraman R, Kellum JA. Defining acute renal failure: the RIFLE criteria. *J Intensive Care Med*. 2007;22:187–193. https://doi.org/10.1177/0885066607299510
21. Berden AE, Ferrario F, Hagen EC, et al. Histopathologic classification of ANCA-associated glomerulonephritis. *J Am Soc Nephrol*. 2010;21:1628–1636. https://doi.org/10.1681/ASN.2010050477
22. Brix SR, Noriega M, Tennstedt P, et al. Development and validation of a renal risk score in ANCA-associated glomerulonephritis. *Kidney Int*. 2018;94:1177–1188. https://doi.org/10.1016/j.kint.2018.07.020
23. Trimarchi H, Barratt J, Cattran DC, et al. Oxford classification of IgA nephropathy 2016: an update from the IgA Nephropathy Classification Working Group. *Kidney Int*. 2017;91:1014–1021. https://doi.org/10.1016/j.kint.2017.02.003
24. Bankhead P, Loughrey MB, Fernández JA, et al. QuPath: open-source software for digital pathology image analysis. *Sci Rep*. 2017;7:16878. https://doi.org/10.1038/s41598-017-17204-5
25. IBM SPSS Statistics for Windows, Version 26.0. IBM Corp. Published 2019. https://www.ibm.com/support/pages/downloading-ibm-spss-statistics-26. Accessed June 1, 2019.
26. Hermsen M, Volk V, Bräsen JH, et al. Quantitative assessment of inflammatory infiltrates in kidney transplant biopsies using multiplex tyramide signal amplification and deep learning. *Lab Investig*. 2021;101:970–982. https://doi.org/10.1038/s41374-021-00601-w
27. Falini B, Flenghi L, Pileri S, et al. PG-M1: a new monoclonal antibody directed against a fixative-resistant epitope on the macrophage-restricted form of the CD68 molecule. *Am J Pathol*. 1993;142:1359–1372.
28. Lau SK, Chu PG, Weiss LM. CD163: a specific marker of macrophages in paraffin-embedded tissue samples. *Am J Clin Pathol*. 2004;122:794–801. https://doi.org/10.1309/QHD6-YFN8-1KQX-UUH6
29. Buechler C, Ritter M, Orsó E, et al. Regulation of scavenger receptor CD163 expression in human monocytes and macrophages by pro- and anti-inflammatory stimuli. *J Leukoc Biol*. 2000;67:97–103. https://doi.org/10.1002/jlb.67.1.97
30. Wang Y, Harris DCH. Macrophages in renal disease. *J Am Soc Nephrol*. 2011;22:21–27. https://doi.org/10.1681/ASN.2010030269
31. Kim M, Lim K, Lee YJ, et al. M2 macrophages predict worse long-term outcomes in human acute tubular necrosis. *Sci Rep*. 2020;10:2122. https://doi.org/10.1038/s41598-020-58725-w
32. Rousselle A, Kettritz R, Schreiber A. Monocytes promote crescent formation in anti-myeloperoxidase antibody-induced glomerulonephritis. *Am J Pathol*. 2017;187:1908–1915. https://doi.org/10.1016/j.ajpath.2017.05.003
33. O'Reilly VP, Wong L, Kennedy C, et al. Urinary soluble CD163 in active renal vasculitis. *J Am Soc Nephrol*. 2016;27:2906–2916. https://doi.org/10.1681/ASN.2015050511
34. Villacorta J, Lucientes L, Goicoechea E, et al. Urinary soluble CD163 as a biomarker of disease activity and relapse in antineutrophil cytoplasm antibody-associated glomerulonephritis. *Clin Kidney J*. 2021;14:212–219. https://doi.org/10.1093/ckj/sfaa043
35. Yokoe Y, Tsuboi N, Imaizumi T, et al. Clinical impact of urinary CD11b and CD163 on the renal outcomes of antineutrophil cytoplasmic antibody-associated glomerulonephritis. *Nephrol Dial Transplant*. 2021;36:1452–1463. https://doi.org/10.1093/ndt/gfaa097
36. Moran SM, Monach PA, Zgaga L, et al. Urinary soluble CD163 and monocyte chemoattractant protein-1 in the identification of subtle renal flare in anti-neutrophil cytoplasmic antibody-associated vasculitis. *Nephrol Dial Transplant*. 2020;35:283–291. https://doi.org/10.1093/ndt/gfy300
37. Zhao L, David MZ, Hyjek E, et al. M2 macrophage infiltrates in the early stages of ANCA-associated pauci-immune necrotizing GN. *Clin J Am Soc Nephrol*. 2015;10:54–62. https://doi.org/10.2215/CJN.03230314
38. Mejia-Vilet JM, Zhang XL, Cruz C, et al. Urinary soluble CD163: a novel non-invasive biomarker of activity for lupus nephritis. *J Am Soc Nephrol*. 2020;31:1335–1347. https://doi.org/10.1681/ASN.2019121285
39. Zhang T, Li H, Vanarsa K, et al. Association of urine sCD163 with proliferative lupus nephritis, fibrinoid necrosis, cellular crescents and intrarenal M2 macrophages. *Front Immunol*. 2020;11:671. https://doi.org/10.3389/fimmu.2020.00671
40. Olmes G, Büttner-Herold M, Ferrazzi F, et al. CD163 M2c-like macrophages predominate in renal biopsies from patients with lupus nephritis. *Arthritis Res Ther*. 2016;18:90. https://doi.org/10.1186/s13075-016-0989-y
41. Bos EMJ, Sangle SR, Wilhelmus S, et al. Use of glomerular CD68+ cells as a surrogate marker for endocapillary

hypercellularity in lupus nephritis. *Kidney Int Rep*. 2022;7: 841–847. https://doi.org/10.1016/j.ekir.2021.12.030

42. Soares MF, Genitsch V, Chakera A, et al. Relationship between renal CD68 infiltrates and the Oxford Classification of IgA nephropathy. *Histopathology*. 2019;74:629–637. https://doi.org/10.1111/his.13768
43. Silva GEB, Costa RS, Ravinal RC, et al. Renal macrophage infiltration is associated with a poor outcome in IgA nephropathy. *Clin (S Paulo)*. 2012;67:697–703. https://doi.org/10.6061/clinics/2012(07)01
44. Hodgin JB, Berthier CC, John R, et al. The molecular phenotype of endocapillary proliferation: novel therapeutic targets for IgA nephropathy. *PLoS One*. 2014;9:e103413. https://doi.org/10.1371/journal.pone.0103413
45. Kim J, Choi S, Lee KH, et al. Tubulointerstitial infiltration of M2 macrophages in Henoch-Schönlein Purpura nephritis indicates the presence of glomerular crescents and bad clinical parameters. *BioMed Res Int*. 2019;2019:8579619. https://doi.org/10.1155/2019/8579619
46. Mantovani A, Allavena P, Marchesi F, Garlanda C. Macrophages as tools and targets in cancer therapy. *Nat Rev Drug Discov*. 2022;16:1–22. https://doi.org/10.1038/s41573-022-00520-5
47. Lim H, Müller N, Herold MJ, et al. Glucocorticoids exert opposing effects on macrophage function dependent on their concentration. *Immunology*. 2007;122:47–53. https://doi.org/10.1111/j.1365-2567.2007.02611.x
48. Ehrchen JM, Roth J, Barczyk-Kahlert K. More than suppression: glucocorticoid action on monocytes and macrophages. *Front Immunol*. 2019;10:2028. https://doi.org/10.3389/fimmu.2019.02028
49. Tillmann F, Grotz W, Rump LC, Pisarski P. Impact of monocyte-macrophage inhibition by ibandronate on graft function and survival after kidney transplantation: a single-centre follow-up study over 15 years. *Clin Exp Nephrol*. 2018;22:474–480. https://doi.org/10.1007/s10157-017-1470-1
50. Grotz W, Nagel C, Poeschel D, et al. Effect of ibandronate on bone loss and renal function after kidney transplantation. *J Am Soc Nephrol*. 2001;12:1530–1537. doi:1046-6673/1207-1530.
51. Naicker SD, Cormican S, Griffin TP, et al. Chronic kidney disease severity is associated with selective expansion of a distinctive intermediate monocyte subpopulation. *Front Immunol*. 2018;9:2845. https://doi.org/10.3389/fimmu.2018.02845
52. Bowe B, Xie Y, Xian H, et al. Association between monocyte count and risk of incident CKD and progression to ESRD. *Clin J Am Soc Nephrol*. 2017;12:603–613. https://doi.org/10.2215/CJN.09710916
53. Jimenez-Duran G, Luque-Martin R, Patel M, et al. Pharmacological validation of targets regulating CD14 during macrophage differentiation. *EBiomedicine*. 2020;61:103039. https://doi.org/10.1016/j.ebiom.2020.103039
54. Bräsen JH, Khalifa A, Schmitz J, et al. Macrophage density in early surveillance biopsies predicts future renal transplant function. *Kidney Int*. 2017;92:479–489. https://doi.org/10.1016/j.kint.2017.01.029
55. Dias CB, Malafronte P, Lee J, et al. Role of renal expression of CD68 in the long-term prognosis of proliferative lupus nephritis. *J Nephrol*. 2017;30:87–94. https://doi.org/10.1007/s40620-015-0252-7
56. Vlasschaert C, Moran SM, Rauh MJ. The myeloid-kidney interface in health and disease. *Clin J Am Soc Nephrol*. 2022;17:323–331. https://doi.org/10.2215/CJN.04120321
57. Engel JE, Chade AR. Macrophage polarization in chronic kidney disease: a balancing act between renal recovery and decline? *Am J Physiol Ren Physiol*. 2019;317:F1409–F1413. https://doi.org/10.1152/ajprenal.00380.2019
58. Schmitz J, Brauns N, Hüsing AM, et al. Renal medullary osmolytes NaCl and urea differentially modulate human tubular cell cytokine expression and monocyte recruitment. *Eur J Immunol*. 2022;52:1258–1272. https://doi.org/10.1002/eji.202149723
59. Eardley KS, Zehnder D, Quinkler M, et al. The relationship between albuminuria, MCP-1/CCL2, and interstitial macrophages in chronic kidney disease. *Kidney Int*. 2006;69:1189–1197. https://doi.org/10.1038/sj.ki.5000212
60. Kidder D, Bray SE, Fleming S. Differences in the frequency of macrophage and T cell markers between focal and crescentic classes of anti-neutrophil cytoplasmic antibody (ANCA)-associated glomerulonephritis. *J Nephropathol*. 2017;6:97–102. https://doi.org/10.15171/jnp.2017.16
61. Hermsen M, de Bel T, den Boer M, et al. Deep learning-based histopathologic assessment of kidney tissue. *J Am Soc Nephrol*. 2019;30:1968–1979. https://doi.org/10.1681/ASN.2019020144
62. Kitamura S, Takahashi K, Sang Y, et al. Deep learning could diagnose diabetic nephropathy with renal pathological immunofluorescent images. *Diagnostics (Basel)*. 2020;10:466. https://doi.org/10.3390/diagnostics10070466
63. Barisoni L, Lafata KJ, Hewitt SM, et al. Digital pathology and computational image analysis in nephropathology. *Nat Rev Nephrol*. 2020;16:669–685. https://doi.org/10.1038/s41581-020-0321-6